

## Magnetic dichroism in the angular distribution of Fe 2*p* and 3*p* photoelectrons: Empirical support to Zeeman-like analysis

Giorgio Rossi

*Laboratorium für Festkörperphysik, ETH-Zürich, CH-8093 Zurich, Switzerland  
and INFN, Dipartimento di Fisica dell' Università di Modena, I-41100 Modena, Italy*

Giancarlo Panaccione

*Institut de Physique, Université de Neuchâtel, CH-2000 Neuchâtel, Switzerland  
and Laboratoire pour l'Utilisation du Rayonnement Electromagnetique, CNRS-CEA-MESR, F-91405 Orsay, France*

Fausto Sirotti

*Laboratoire pour l'Utilisation du Rayonnement Electromagnetique, CNRS-CEA-MESR, F-91405 Orsay, France*

Silvano Lizzit, Alessandro Baraldi, and Giorgio Paolucci

*Sincrotrone Trieste, S.c.p.A., Padriciano 99, I-34012 Trieste, Italy*

(Received 22 July 1996; revised manuscript received 29 October 1996)

We report on the measurements and analysis of Fe 2*p* magnetic dichroism in the angular distribution of the photoelectrons from remanently magnetized Fe(100) surfaces with unpolarized, monochromatized, x rays of 1486 eV energy, and with linearly polarized synchrotron radiation of 800 eV energy. The analysis of the dichroic photoemission intensity in the two experiments verifies the applicability of the atomic photoionization model which provides a consistent understanding of the differences between photoemission experiments with unpolarized and linearly polarized radiation. A comparison of the Fe 2*p* and Fe 3*p* dichroism spectra allows us to discuss, on an empirical basis, the validity of a Zeeman-like interpretation of Fe 3*p* hole sublevels connected to the observed magnetic dichroism in photoemission. [S0163-1829(97)02514-9]

### INTRODUCTION

Magnetic dichroism in photoemission represents an important experimental development in the field of surface and interface magnetism.<sup>1-14</sup> Both circularly polarized radiation and linearly polarized radiation from synchrotron radiation (SR) sources can be exploited to perform dichroism experiments that are sensitive to the magnetic order of surfaces and interfaces. The use of linearly polarized radiation and unpolarized radiation requires angular selection of the photoelectrons in order to define a chirality between the vectorial quantities of the photoemission experiment. Magnetic dichroism in the angular distribution of photoelectrons (MDAD) with unpolarized light as well as with linearly polarized light (LMDAD) have been performed mostly on shallow core levels and on valence bands of the ferromagnetic transition metals and of the rare earths.<sup>15</sup>

The basic understanding of MDAD, with any kind of light polarization, is provided by the theory of photoionization from atomic states.<sup>13</sup> The angular distribution of the photoelectrons, for sufficiently high final state energies, has structures which identify the initial state wave functions, i.e., the magnetic core hole sublevels, which are non degenerate when the excited atom carries a magnetic moment. The result is that the line shapes of, e.g., the 2*p* or 3*p* photoemission peak of the ferromagnetic transition metals are different for different chiral experiments.<sup>9,11,13</sup> The (L)MDAD effect averages out only if (a) full angular integration of the photoemission current is performed, (b) the ferromagnet is di-

vided in randomly oriented domains (demagnetized state), and (c) the sample temperature exceeds the Curie temperature. Otherwise (L)MDAD is a large effect which can reach 45% of the Fe 3*p* intensity.<sup>12</sup>

Rossi *et al.* first proposed a semiempirical analysis of the LMDAD intensities of Fe 3*p* and Co 3*p* using a six peak fit of the field-averaged and dichroic intensities.<sup>4</sup> The next step was the comparison of the chirality-dependent peak intensities with the intensity ratios predicted by atomic photoionization theory for atomic 3*p* *m<sub>j</sub>* sublevels in the directions defined by the experimental geometry.<sup>5</sup> A similar procedure was proposed first by Ebert *et al.*<sup>7</sup> for the analysis of magnetic dichroism in photoemission of Fe 2*p* core levels with circularly polarized radiation.<sup>1</sup> As a result the 3*p* photoemission was described by six components: two spin orbit split components ( $J=3/2$ ,  $J=1/2$ ) further split in individual *m<sub>j</sub>* sublevels, differing from the level splitting of the anomalous Zeeman effect only in the inversion of the energy order of the sublevels of the  $J=1/2$  doublet.<sup>5,7</sup> The (L)MDAD effect is connected to the *orientation* of the magnetic moments.<sup>11</sup> This analysis suggested the use of LMDAD as a surface magnetometer: experiments have shown that the magnitude of the LMDAD asymmetry relates directly to the magnetic order parameter, whilst the splitting between the sublevels relates to the value of the magnetic moment of the photoionized atoms.<sup>12,16</sup> More recently a different effect has been measured between *magnetic field averaged photoemission* experiments with variable chirality (magnetic field averaged photoemission dichroism):<sup>17</sup> nonzero spectral differences are

measured which are due to the *alignment* of the magnetic moments along the magnetic quantization axis. MFAPD is independent on the value of magnetization (including zero magnetization), and it is again well explained by the atomic model.<sup>17</sup> The quantitative analysis of the Fe 3*p* LMDAD and MFAPD spectra raises several questions on the description of the core hole multiplet: (a) the spin orbit and the exchange splitting in Fe 3*p* have about the same magnitude ( $1.05 \pm .05$  eV) and a Zeeman like picture of the 3*p* core hole, treating the exchange splitting as a perturbation of the spin orbit splitting scheme is not justified *a priori*; (b) it has been noted<sup>11</sup> that the measured  $J=1/2$  contributions to the Fe 3*p* spectra are less intense than expected, and that the precise assignment of their energies is difficult; (c) the  $m_{j=1/2}$  energies are expected to vary according to the ratio between the energy values of the exchange and spin-orbit interactions since these sublevels are not pure spin-orbit states.<sup>9</sup> The possible presence of satellites of the main final state peaks was also questioned.<sup>18,19</sup> Experimentally it has been shown that Fe 3*p* spectra present negligible satellite intensity outside of the main peak, contrary to Ni and Co 3*p*.<sup>20</sup> However, satellites could be hidden in the highly asymmetric line shape of Fe 3*p*, therefore affecting the sextuplet analysis.

An interesting experimental extension of this research is to measure the Fe 2*p* core levels where the large spin-orbit interaction within the open core widely separates the final state photoemission intensity arising from the  $2p_{3/2}$  and  $2p_{1/2}$  terms. *A priori* one can consider the analysis of the Fe 2*p* photoemission experiment easier since the Zeeman-like description is well adapted to it (the exchange splitting being of the order of 7–8 % of the spin orbit splitting).<sup>7,9,21</sup> Hillebrecht *et al.*<sup>21</sup> have recently reported on a spin resolved LMDAD Fe 2*p* experiment which clearly shows the presence of LMDAD features both on the  $2p_{3/2}$  and  $2p_{1/2}$  peaks, and also in between the main peaks. The  $2p_{3/2}$  data were fitted by sublevel components, following the philosophy of Ref. 5, obtaining a quadruplet of levels split by 0.5 eV for the  $2p_{3/2}$  component. This value is 50% larger then previously reported for the Fe 3*p*,<sup>5</sup> which fact must be understood since if the same description holds for both 2*p* and 3*p* photoemission peaks, one expects a similar exchange splitting for both  $2p_{3/2}$  and  $3p_{3/2}$  multiplets. Here we present and discuss the results of Fe 2*p* and Fe 3*p* (L)MDAD experiments which were performed with an unpolarized, monochromatized, Al *Kα* x-ray source, as well as with linearly polarized SR from the SuperESCA beam line of the ELETTRA laboratory at Trieste. The 2*p* and 3*p* (L)MDAD data are analyzed in a consistent way, which allow to discuss the accuracy of the Zeeman-like model for the analysis of magnetic dichroism in photoemission.

## EXPERIMENT

Fe(100) surfaces were prepared by Ar<sup>+</sup>-ion sputtering and annealing a [100]-oriented iron single crystal (3% Si-stabilized) mounted to close the gap of a soft iron yoke and clamped to a six degree of freedom manipulator in the SuperESCA spectrometer at the ELETTRA SR laboratory of Trieste.<sup>22</sup> The iron single crystal could be magnetized in-plane to saturation by passing a direct current through a

winding around the soft iron yoke. The magnetization vector **M** could be directed along the normal to the photoemission reaction plane (i.e., along the vertical direction) either up or down, by reversing the sign of the current pulses. All the data were measured in remanence conditions at temperatures of 150 K or 300 K. The photoemission current was selected at normal emission by a 150 mm-diameter hemispherical electrostatic electron energy analyzer, with an angular acceptance of  $\pm 2^\circ$ . The two photon sources used for the experiments were (1) a focused and monochromatized Al *Kα* source delivering an unpolarized photon beam of  $h\nu=1486$  eV impinging onto the sample in the horizontal plane at an angle  $\Theta = -40^\circ$  with respect to the **k** vector selected by the electron analyzer and (2) monochromatic linearly polarized undulator SR of  $h\nu=800$  eV and of  $h\nu=198$  eV impinging the sample at  $\Theta = +40^\circ$  with respect to **k** with the electric vector **e** in the horizontal plane, i.e., in *p*-polarization configuration. Referring to Fig. 1, the geometry of the experiments with the unpolarized x-ray photons is the mirror image, about the **Mk** plane, of the geometry of the experiments with linearly polarized synchrotron radiation. The plus/minus feature of the measured MDAD and LMDAD dichroism is therefore opposite. The overall energy resolution of the two experiments on Fe 2*p* was of the order of 300 meV.

## RESULTS

The Al *Kα* x-ray photoemission spectra measured in the two mirror geometries indicated in the inset are presented in Fig. 1(a), along with the difference curve ( $\mathbf{M}_{\text{up}} - \mathbf{M}_{\text{down}}$ ) showing the MDAD effect in Fig. 1(b). Obeying to the sum rule on the photoemission intensity that must hold when integrating over an extended energy range, including regions well outside of the main peaks, the two spectra have been normalized to equal total intensity. Such normalization procedure is also justified by the integral value of the MDAD dichroism, which is nearly zero. The photoemission intensity depends on **M** both in between the  $2p_{3/2}$  and  $2p_{1/2}$  peaks and at lower kinetic energy than the  $2p_{1/2}$  peak. The MDAD asymmetry is defined as  $A_{(L)MDAD} = (I_{\text{up}} - I_{\text{down}}) / (I_{\text{up}} + I_{\text{down}})$ , where  $I_{\text{up (down)}}$  are the photoelectron spectral intensities obtained with the magnetization in the upward (up) or downward (down) directions. Two MDAD asymmetries are shown in Fig. 1(c): the solid line is the experimental asymmetry, obtained by dividing the MDAD difference by the sum of the as measured spectra. This curve is useful to estimate the measurable size of the dichroism in an experiment, but cannot be used to estimate the true spectral asymmetry, because the background of the photoemission spectra is included. The dashed curve represents the spectral asymmetry, obtained by dividing the MDAD difference by the sum of the two spectra after an integral background subtraction. This curve is very noisy wherever the spectral intensity becomes small: it shows that  $A_{MDAD_{2p_{1/2}}} \approx 3/4 A_{MDAD_{2p_{3/2}}}$ . Several structures are shown by arrows: their energy position correspond to the features readily observable also in the MDAD difference, and some of these do have a high asymmetry. The MDAD difference and experimental asymmetry curves are in excellent agreement with the LMDAD data obtained with  $h\nu=879$  eV by Hillebrecht *et al.* in Ref. 21.

The dichroism measured at the  $2p_{3/2}$  peak consists in a

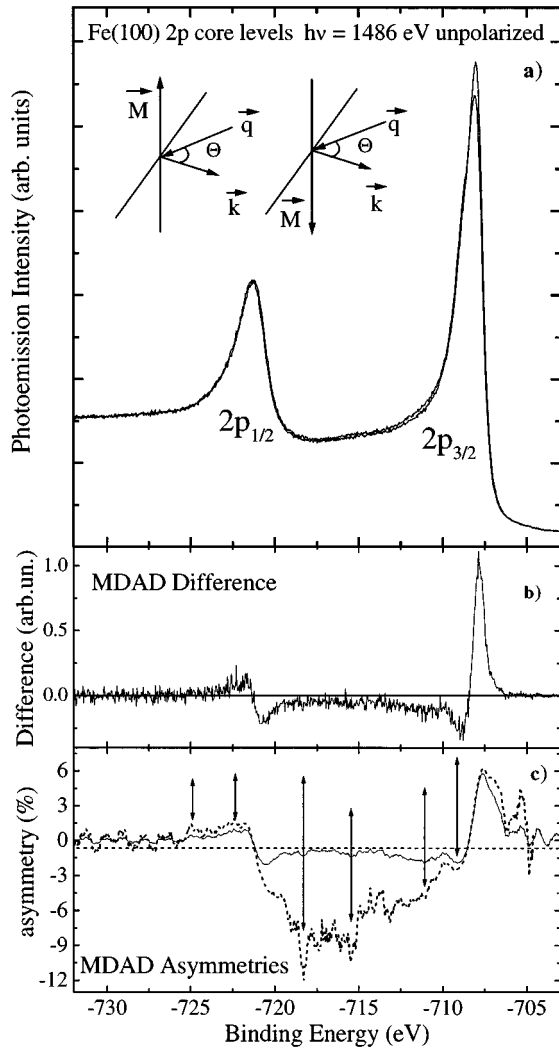


FIG. 1. (a) Fe  $2p$  photoemission spectra of remanently magnetized Fe(100) as measured with unpolarized Al  $K\alpha$  x-rays in the two mirror chiral geometries shown in the inset.  $\mathbf{M}$  is the magnetization vector,  $\mathbf{k}$  is the photoelectron momentum vector, and  $\mathbf{q}$  is the vector defining the propagating photon beam. The magnetization dependent spectra have been normalized to equal total intensity. (b) MDAD difference. (c) MDAD experimental (continuous line) and spectral (dashed line) asymmetry curves, as defined in the text, after filtering of the statistical noise by five point averaging. The arrows indicate weak features appearing near to and in between the main peaks.

plus/minus feature centered at 708.28 eV,  $\sim 1$  eV wide, followed, at lower kinetic energies, by a modulated negative asymmetry (the absolute sign depends on the chirality of the experiment) showing distinct features at 710.8 eV and 715.4 eV. The extrema of the MDAD experimental symmetry are +6% and -2% for the  $J=3/2$  peak, and 1% and -2% for the  $J=1/2$  peak. The dichroism at the  $2p_{1/2}$  main peak is of opposite sign, centered at 721.5 eV of binding energy and has a similar width although the plus feature is not prominent. The small value of the dichroism at higher binding energies than the  $2p_{1/2}$  peak is understood as due to the large  $2p_{3/2}$  dichroism background, onto which the  $2p_{1/2}$  dichroism

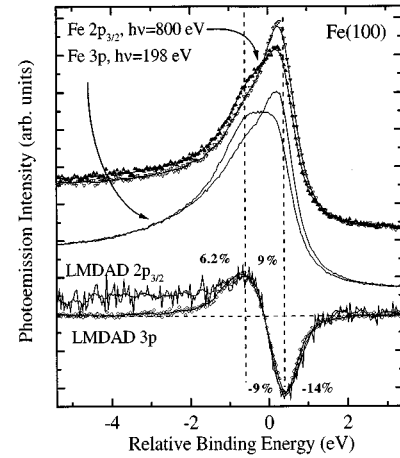


FIG. 2. Fe  $2p_{3/2}$  (up full and down open triangles) and Fe  $3p$  (continuous lines) magnetization dependent spectra and LMDAD curves obtained with linearly polarized SR of  $h\nu=800$  eV and  $h\nu=198$  eV, respectively. The spectra are traced on a relative electron energy scale for the comparison of lineshapes and the LMDAD spectra are normalized to the same height for graphical comparison. Vertical dashed bars indicate the extrema of the dichroism curves. The LMDAD asymmetry values corresponding to Fe  $2p_{3/2}$  (solid curve through the data and smoothed curve) are -9% and +6.2% and for Fe  $3p$  (open diamonds and smoothed curve) are -14% and +9%. The LMDAD asymmetry is a function of the photon energy.

is superimposed. The  $2p_{3/2}$  photoemission peak has a prominent shoulder at 708.9 eV which coincides with one extremum of the MDAD curve. The Fe  $2p_{3/2}$  magnetization dependent spectra and the relative LMDAD curves measured with linearly polarized SR of  $h\nu=800$  eV are presented in Fig. 2 along with the Fe  $3p$  spectra and LMDAD as measured with  $h\nu=198$  eV. The lineshape of Fe  $2p$  spectra at higher photon energy (data were measured up to 1300 eV) with linearly polarized radiation does not change within our sensitivity. The extrema of the LMDAD asymmetry for Fe  $2p_{3/2}$  are +6.2% and -9%. The extrema of the LMDAD asymmetry for Fe  $3p$  at 198 eV are +9% and -14%. The two LMDAD curves show very similar width, indicated by the vertical dashed bars, and line shape.

## DATA ANALYSIS

### Fe $2p$ (L)MDAD

The energy positions of the inflection points of the (L)MDAD curves in the  $2p_{3/2}$  and  $2p_{1/2}$  spectra indicate the center of the main multiplets and allow for an accurate estimate of the spin orbit splitting of the  $2p$  spectrum, which is  $13.01 \pm 0.03$  eV. Small peaks and a continuum of dichroic intensity appears in between the  $J=3/2$  and  $J=1/2$  peaks and at higher binding energy than the  $2p_{1/2}$  peak. Some weak features are identified by arrows in the (L)MDAD difference curve in Figs. 1(b) and 1(c). A detailed and quantitative analysis of the dichroism in the spectrum outside of the main peaks is difficult since one should take into account that (a) the intensity of the weak features could depend on photon energy and emission angle, as shown in Ref. 21 and (b) the

spectral asymmetry values of the weak features are strongly dependent on the background subtraction procedure. However, we found that the background subtraction procedure may vary the relative intensity but cannot suppress the presence of these weak features. The weakly structured dichroic intensity in between the main peaks suggests the presence of discrete final state configurations (satellites) rather than of a continuum of scattering states (background), but this point cannot be conclusively addressed on the basis of the present experiment. On the other hand, the very high tails towards higher binding energy of the main photoemission peaks should be attributed to satellites. In fact the genuine peak width of the  $2p_{3/2}$  and  $2p_{1/2}$  main peaks is identified by the simple atomiclike shape of the large plus-minus (L)MDAD features which identify the full width of the  $J=3/2$  quartet and  $J=1/2$  doublet, respectively.<sup>5,11,13</sup> Also from Fig. 2 one can see that the width of the  $2p_{3/2}$  LMDAD is  $1.05 \pm 0.02$  eV, which is the same, within our accuracy as for the Fe  $3p$  LMDAD. A quartet of  $m_j$  sublevels with a total width of  $1.05 \pm 0.02$  eV cannot account for the extended tail of the Fe  $2p_{3/2}$  photoemission spectra, not even by assuming *large* Doniac-Sunjic<sup>23</sup> type asymmetry factors for the individual  $m_j$  peaks. We attribute the high energy tail intensity to unresolved satellites. Since the exact energy position and line shape of these satellites cannot be retrieved from the data, we analyze the photoemission line shape by analyzing first the (L)MDAD line shape, using the LMDAD width as the “fingerprint” of the position of the  $m_j = \pm 3/2$  peaks. The energy width of the  $2p_{3/2}$  (L)MDAD as measured at the two energies is identical, within experimental error, as shown in Figs. 3(a) and 3(b). The  $\mathbf{M}$  averaged spectrum as obtained with unpolarized Al  $K\alpha$  radiation and the fit are shown in Fig. 4. The hypothesis of the fit of the  $2p_{3/2}$  spectrum is that a quartet of sublevels of identical line shape with the energy constrains set by the MDAD peak positions and by the equal splitting intervals between the sublevels (like in the Zeeman splitting) should represent the photoemission intensity of the  $m_j$  core hole sublevels of the  $J=3/2$  multiplet as well as the dichroism. The parameters of the best fit are listed in the caption of Fig. 5. The fitted peak accounts for 85% of the total intensity. The residual intensity under the tail (dotted line) is compared to a replica of the spectrum shifted by  $-1.43 \pm 0.03$  eV. We describe this residual intensity as arising from a satellite which would not be resolved in absence of the MDAD spectrum. Figure 5 compares the fit of the  $\mathbf{M}$  dependent Al  $K\alpha$  and SR data. We obtain that the same set of multiplet parameters fit both the spectra measured with linearly polarized SR of  $h\nu=800$  eV [Fig. 4(a)] and with unpolarized radiation of  $h\nu=1486$  eV [Fig. 4(b)] which justifies our comparison of spectra obtained with different photon energies. Figure 5(c) shows the fit of the Fe  $2p_{1/2}$  peak. The field averaged Fe  $2p_{3/2}$  spectra from the two experiments are compared in Fig. 3(c). The nonzero experimental difference represents the MFAPD effect. It is compared with the atomic model calculation of MFAPD using the fitted sextuplet.<sup>17</sup>

### Fe $3p$ (L)MDAD

The fitting of the Fe  $3p$   $\mathbf{M}$ -averaged spectrum and LMDAD with a sextuplet of sublevels is shown Fig. 6(a),

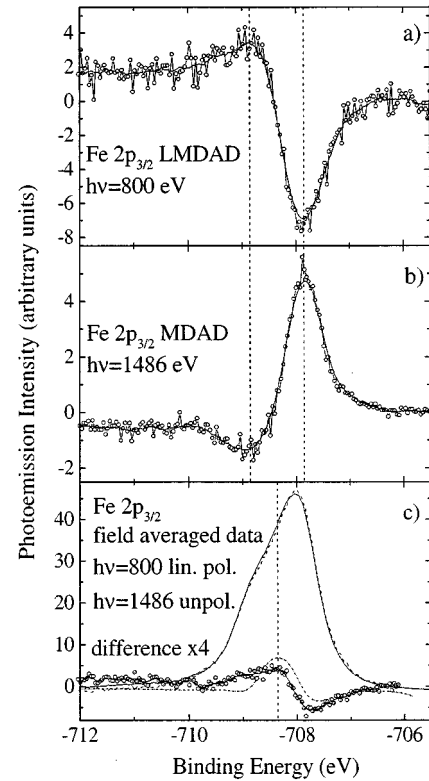


FIG. 3. (a) Fe  $2p_{3/2}$  LMDAD raw data (open symbols) and smoothed data; (b) Fe  $2p_{3/2}$  MDAD data (open symbols) and smoothed data; vertical dashed lines indicate that positions of the maxima are identical, within experimental error. (c) Fe  $2p_{3/2}$  MFAPD effect between Al  $K\alpha$  and SR experiments. The dot-dashed line is obtained by calculating Eq. (4) of Ref. 17 and applying the results to the sextuplet of sublevels shown in Fig. 4.

following the procedure discussed in Ref. 5. The energy position of the  $J = \pm 3/2$  sublevels is fixed by the peaks of the LMDAD curve, the other constraints are the number of sublevels (6), the regular spacing, and the constant peak shape within the  $J=3/2$  multiplet. The  $J=1/2$  sublevels are broader than the  $J=3/2$  sublevels. The individual peaks of the sextuplet of Fig. 6(a) are multiplied for the appropriate cross section ratios calculated within the atomic model for the six  $m_j$  magnetic sublevels of a  $3p$  core hole<sup>5,11</sup> to generate the curves that are compared to the experimental LMDAD in Fig. 6(b). The dot-dashed line is obtained by considering only the  $J=3/2$  quartet. The dashed line is obtained by adding the signals from the six sublevels ordered according to the anomalous Zeeman effect. The continuous line, which best approximates the experimental LMDAD curve, is obtained by inverting the order of the  $J=1/2$  sublevels.

## DISCUSSION

### Unpolarized and linearly polarized dichroism

The  $2p$  spectra measured with SR have more sharply marked shoulders identifying the  $m_j = -3/2$  sublevel than the unpolarized x-ray photoemission spectra, as seen from Figs. 3 and 5. The overall energy resolution of the spectra measured with SR and with Al  $K\alpha$  x rays is similar, as can be easily estimated from the slope and curvature of the lead-

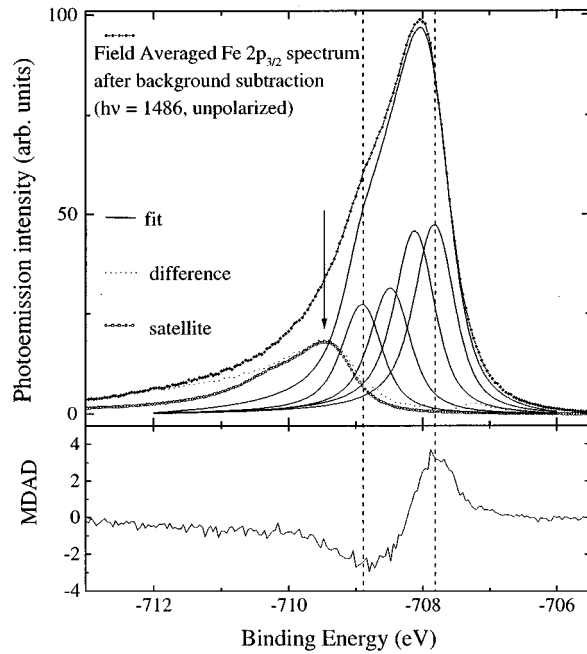


FIG. 4. Top: Fe  $2p_{3/2}$  field-averaged spectrum after integral background subtraction (full symbols) and fit (solid lines) with six peaks. The large tails extend the intensity well below the shoulder and the width of the MDAD spectrum (bottom panel). The main peak, identified by the MDAD spectrum, accounts for  $\sim 85\%$  of the total Fe  $2p_{3/2}$  intensity. The residual (dotted line) is compared to a replica of the spectrum, reduced in intensity and shifted by  $-1.43$  eV. Bottom: The MDAD difference curve from the raw data of Fig. 1 is shown to better identify the position and the width of the multiplets.

ing edges of the main peaks. In agreement with previous experiments,<sup>6,15</sup> and with the atomic model,<sup>11</sup> the magnitude of the MDAD effect measured with unpolarized radiation is reduced with respect to the magnitude of the LMDAD effect measured by linearly  $p$ -polarized SR. The reduction factor would be exactly  $1/2$  for experiments using the same photon energy. This fact follows from the understanding of the MDAD measured with unpolarized light as being due only to the 50% of the x-ray intensity which acts effectively as in-plane linearly polarized radiation defining a  $p$ -polarized experiment. The remaining 50% of the x-ray intensity is effectively acting as linearly polarized radiation perpendicular to the reaction plane, defining a  $s$ -polarized experiment. The  $s$ -polarized intensity generates a nondichroic spectrum, since all vectors are coplanar in the  $\mathbf{Mk}$  (vertical) plane, as already shown by Roth *et al.* in an experiment with vertical linearly polarized SR<sup>2</sup>. The nondichroic spectrum has a line shape which is *different* from the  $\mathbf{M}$  average of the two dichroic spectra. This explains the reduced shoulders in the Al  $K\alpha$  x-ray Fe  $2p_{3/2}$  peak which is the sum of 50% nondichroic and 50%  $\mathbf{M}$ -averaged-dichroic spectral intensities, with respect to the 100% dichroic  $\mathbf{M}$ -averaged SR spectrum. In a recent Fe  $3p$  photoemission experiment with variable chirality it has been shown that the difference between magnetic field averaged photoemission spectra obtained with different chiralities is nonzero.<sup>14</sup> This effect (MFAPD) is re-

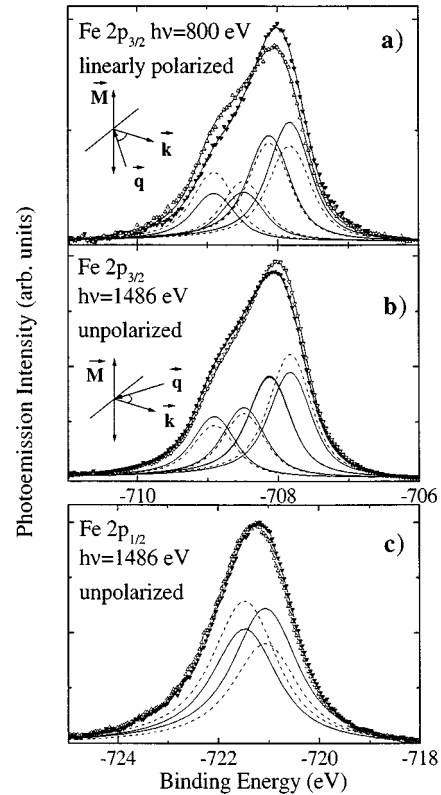


FIG. 5. Best fit of the  $\mathbf{M}$  dependent Fe  $2p_{3/2}$  and Fe  $2p_{1/2}$  spectra by  $m_j$  sublevels. The quartet which fits both the linearly polarized and unpolarized Fe  $2p_{3/2}$  data has a total width of 1.06 eV and interval between adjacent peaks of  $0.35 \pm 0.03$  eV. The fitting functions are Gaussian-Lorentzian line shapes with 0.4 eV gaussian width, 0.45 eV Lorentzian width, and a Sunjic-Doniac asymmetry parameter of 0.05, which is an accepted value for metals. The Fe  $2p_{1/2}$  data are fit by a doublet separated by 0.43 eV, with Lorentzian width of 1 eV and no asymmetry (which is negligible at these large Lorentzian values). The fitting parameters were optimized on the (L)MDAD spectra: the same quartet of levels fits the Fe  $3p$  LMDAD (see text and Fig. 7). Open up triangles and dashed lines are for  $\mathbf{M}_{\text{up}}$  data and fitted peaks. Full down triangles and continuous lines are for  $\mathbf{M}_{\text{down}}$ .

lated to the *alignment* of the magnetic moments and is observed whenever a well defined magnetic quantization axis exists, independent of  $\mathbf{M}$  averaging over  $180^\circ$  domains, or antiferromagnetic ordering. The difference between the magnetic field averaged Al  $K\alpha$  and SR Fe  $2p_{3/2}$  spectra shown in Fig. 3(c) represents the MFAPD effect. The calculation of the MFAPD curve using the atomic model [Eq. (4) of Ref. 17)] applied to the fitted sextuplet of Fig. 4 is shown as a dot-dashed line: it provides the explanation of the nonzero experimental difference. This last results completes the understanding of the Fe  $2p$  chiral photoemission from magnetically ordered iron surfaces, and sets a new, independent, constraint to the fitting of the sextuplet. The presence of both LMDAD and MFAPD effects has been shown here by comparison with linearly polarized synchrotron radiation spectra. It follows that, in the case of zero (L)MDAD effect, the spectrum for a truly demagnetized sample can always be

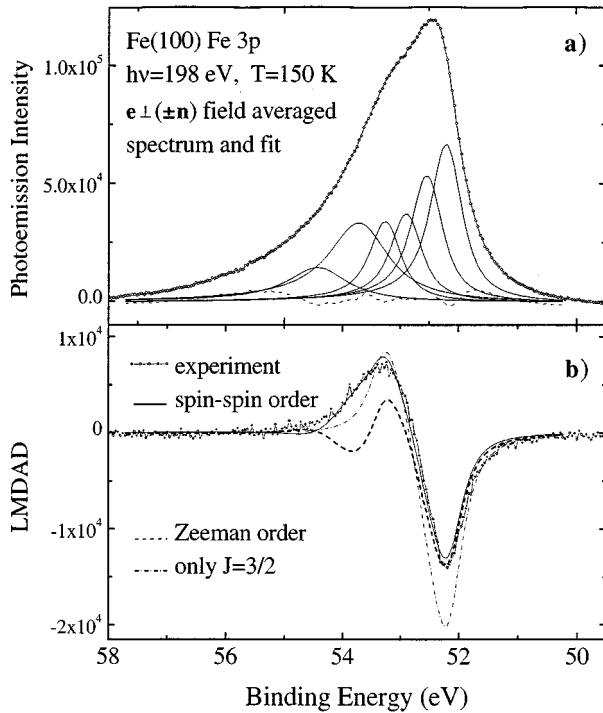


FIG. 6. (a) Fe  $3p$   $\mathbf{M}$  field averaged spectrum, obtained with  $h\nu = 198$  eV, and fitting sextuplet. The dashed line represents the residual difference between data and fit. (b) Experimental LMDAD curve (symbols) and LMDAD calculations obtained by multiplying the individual intensities of the six fitting peaks by the cross section ratios predicted by the atomic model for the six  $m_j$  magnetic sublevels of a  $3p$  core hole. The dot-dashed line is the average of the contributions of just the  $J=3/2$  quartet. The dashed line is the average of the full sextuplet contributions ordered according to the anomalous Zeeman effect. The continuous line, which approximates the data best, is the average of the sextuplet when the order of the  $J=1/2$  sublevels is inverted.

recognized from that of a sample with  $180^\circ$  domains, or of an antiferromagnetically ordered surface by comparing the  $\mathbf{M}$ -averaged  $2p$  (or  $3p$ ) core photoemission spectra obtained for different chiralities. If a magnetization axis exists, then the MFAPD difference is nonzero. It also results that if the fit is constrained by the LMDAD (and/or MFAPD) curves, then no specially large broadening of the peaks is observed, and the exchange splitting of adjacent  $J=3/2$  sublevels is of  $\sim 0.35$  eV.

#### Fe $2p$ vs Fe $3p$ : validity of the Zeeman-like analysis

Spin orbit interaction splits the Fe  $2p$  final state in  $1/2$  and  $3/2$  multiplets which are measured at  $13.01 \pm 0.02$  eV energy separation. From the related photoabsorption experiments on the  $2p$  core levels and from the successful application of the sum rules for the circular magnetic dichroism,<sup>25</sup> there is independent evidence that the  $3/2$  and  $1/2$  multiplets of Fe do not show overlapping intensities in the final state. It is therefore justified in this case to treat the exchange splitting as a perturbed level scheme due to the Weiss field (or exchange field) acting on the core hole levels. The analysis of the

dichroism on the Fe  $2p_{3/2}$  peak is greatly simplified with respect to the case of Fe  $3p$ , since in the present case only four sublevels contribute. The hypothesis that the  $J=3/2$  magnetic sublevels are separated by equal energy intervals is also a better approximation in this case. It is important to remark that in the present data, as well as in previous reports of Fe  $2p$  dichroism, one clearly sees satellite intensity of the iron  $p$  photoemission.<sup>24</sup> The Fe  $3p$  peaks and dichroism do not show (differently from Ni and Co spectra) any satellite intensity.<sup>20</sup> The  $\sim 25\%$  reduced value of the (peak to peak) dichroism asymmetry corresponding to the Fe  $2p_{1/2}$  peaks, with respect to Fe  $2p_{3/2}$ , is determined by two factors: (1) the smaller atomic effect (smaller angular cross section ratios<sup>11</sup>) and (2) the large increase of lifetime broadening for the  $1/2$  peaks which is found in a doubled value of Lorentzian line shape in the fits.<sup>5,20</sup>

In  $3p$  photoemission the spin orbit splitting is  $1.05 \pm 0.05$  eV as measured in nonmagnetic iron silicide,<sup>26</sup> which means that the ratio between exchange splitting and spin-orbit splitting is  $\sim 1$  and one should expect an intermediate coupling description to be required. In the Zeeman-like model in fact the  $3p_{3/2}$  and  $3p_{1/2}$  sublevels do partially overlap. Also the splitting of the  $J=3/2$  multiplet may not lead to regularly spaced sublevels as in the Zeeman-like picture.<sup>9</sup> Previous analysis of the  $3p$  LMDAD spectra with the atomic model was based on a simple sextuplet of levels where each  $J$  multiplet was split in  $m_j$  sublevels in a Zeeman-like scheme.<sup>5,13,6</sup> The main feature of the LMDAD spectrum was found to derive from the  $m_j = \pm 3/2$  sublevels which determine the overall shape of the LMDAD curve, and its energy width. The  $3p$  spectra were found to be sensitive to the energy ordering of the  $J=1/2$ ,  $m_j = \pm 1/2$  sublevels,<sup>7,5,12</sup> but were little affected by the exact energy position of them, which in fact appeared to vary with photon energy, energy resolution, and angular resolution of the spectra, unlike the  $J=3/2$  sublevels. A many body calculation of Fe  $3p$  dichroism confirmed the grid of 6 sublevels, split by the effective exchange field, and ordered in general agreement with a Zeeman-like scheme (with inverted ordering for the  $J=1/2$  doublet).<sup>10</sup> From the analysis of Fig. 6 it appears that the full sextuplet, with inverted  $J=1/2$  splitting, is indeed capable of reproducing the experimental dichroism. Strictly speaking the results of Fig. 6 show that the chirality dependence of the intensity of the tail of the  $3p$  peak is the same as predicted by the atomic theory for  $J=1/2$  sublevels when applied to the two “ $J=1/2$ ” fitted peaks. It remains that the exact spectral weight and distribution of the  $J=1/2$  are not well defined: the degree of overlap of  $J=3/2$  and  $J=1/2$  multiplets cannot be reliably determined by the sextuplet fitting procedure, and the tail might contain contributions from unresolved satellites.

A comparison of the  $2p_{3/2}$  and  $3p$  LMDAD spectra can be used to empirically assess the magnitude of the effects connected with the overlapping  $J=1/2$  contributions to the  $3p$  LMDAD dichroism, independently from the sextuplet model. We adopt a fully empirical procedure to simulate, using the raw  $2p$  photoemission spectra and LMDAD spectra, the  $3p$ -like spectrum by graphically reducing the spin orbit splitting of the  $2p$  spectra to the  $1.05$  eV value which is appropriate for Fe  $3p$ . This procedure produces an artificial

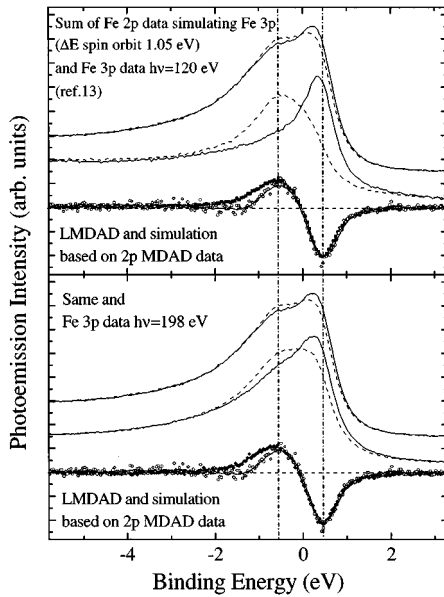


FIG. 7. (a) Comparison of the Fe 3*p* spectra measured with  $h\nu = 120$  eV (Ref. 12) and a simulation obtained from the Fe 2*p* spectrum by graphically reducing the spin-orbit splitting to the proper value for Fe 3*p* (1.05 eV). The top pair of curves is the simulated Fe 3*p* spectra. The central pair is the Fe 3*p* true spectra as measured with  $h\nu = 120$  eV. In both pairs the dashed curve is for  $M_{\text{up}}$  and the continuous curve is for  $M_{\text{down}}$ . The bottom pair of curves represent the simulated LMDAD curve (solid line through the open circles) and the difference of the  $h\nu = 120$  eV data (solid squares). The midpoint of the LMDAD spectra coincide, but the positive LMDAD peak extends to higher binding energies than in the simulated spectrum. (b) Same as in (a), but with the Fe 3*p* experimental spectra as measured with  $h\nu = 198$  eV.

spectrum which is interpretable in the Zeeman-like model since its ingredients are just the Fe 2*p* photoemission curves, and no interaction between  $p_{3/2}$  and  $p_{1/2}$  is introduced. The result of this cut-and-paste manipulation of the 2*p* spectra is shown in Fig. 7 where it is compared to the genuine Fe 3*p* LMDAD data as measured with two photon energies, representative of many experiments. The shape of the simulated peaks and of the real data are in good general agreement if one takes into account that the LMDAD asymmetry is reduced at high photon energy. Most important is the comparison between the LMDAD curves, which have been normalized to the same peak to peak intensity difference. The artificial LMDAD spectrum width remains basically identical to that of Fe 2*p* $_{3/2}$ , and it compares favorably, within an error of 3%, to the Fe 3*p* LMDAD as measured with two different experimental apparatuses and two different photon energies. The general shape and the energy width of the Fe 3*p* LMDAD curve do not show any major effect due to intermediate coupling. The accuracy limit of this empirical Zeeman-like treatment and the “error bar” connected to the 3*p* LMDAD width value can be traced in the extra LMDAD signal at lower kinetic energy which is present in the Fe 3*p* data between  $-2$  and  $-0.5$  eV and is not found in the simulation. The fact that the LMDAD splitting is basically identical in Fe 2*p* $_{3/2}$  and Fe 3*p* is a confirmation that the

same LMDAD analysis is appropriate for both core levels, and that the atomic model in the Zeeman-like approximation is a useful guideline to understand the 3*p* spectra. An accurate analysis of the (L)MDAD dependence on the magnetic moment requires measuring absolute standards. We believe that this demands truly bulk sensitive photoemission experiments, i.e., exciting photoelectron final state energies of the order of several KeV. All of the present data, as well as those presented in the literature, are affected by a poorly defined degree of surface and subsurface sensitivity which makes possible to discuss only relative changes of LMDAD within a given experiment at a fixed energy and geometry as a function of sample treatment, but do not allow for more quantitative and general conclusions.

## CONCLUSIONS

We summarize the results as follows. (1) MDAD on Fe 2*p* core levels can be measured very accurately by monochromatized unpolarized x-ray sources, e.g., in a laboratory environment. The MDAD data are fully consistent with the LMDAD data measured by linearly polarized synchrotron radiation. The magnetization dependent spectra are different though when they are measured by unpolarized light or with linearly polarized light. This is due to the sum of dichroic and nondichroic intensities arising from the *p*-polarized-like and *s*-polarized-like experiments which are simultaneously done when measuring photoemission in chiral geometry with unpolarized light. We have shown that the difference in line shape of the *s*-polarized-like experiment and the field averaged *p*-polarized experiment is explained by the MFAPD effect due to the alignment of the core holes along the magnetization axis. (2) The measured satellite intensity for Fe 2*p* core level photoemission amounts to a small fraction of the total intensity under the main peaks, but it determines the high tails of the spectra. The (L)MDAD spectra can be fitted with just one quartet for the 2*p* $_{3/2}$  peak, and a doublet for the 2*p* $_{1/2}$  peak. (3) The 2*p* $_{3/2}$  LMDAD width is the same as the Fe 3*p* LMDAD within experimental error. The same quartet can be used unmodified, with the addition of the 1/2 doublet, to fit the 3*p* spectra and LMDAD. This fact shows that the Zeeman-like approach followed in the past when describing the Fe 3*p* data with six peaks and attributing  $m_J$  character to those peaks on the basis of the intensity ratios predicted by photoionization theory is justified a posteriori by the evident dominant role of the  $J=3/2$  multiplet in the Fe 3*p* photoemission dichroism.

Although at this stage the analysis remains at the qualitative level, and insofar limited to the case of iron, it is promising that the 3*p* LMDAD splitting is little affected by intermediate coupling and can therefore be used, as well as the Fe 2*p* $_{3/2}$  LMDAD, for monitoring relative changes of the magnetic moments of the photoexcited atoms at surfaces and interfaces.

## ACKNOWLEDGMENTS

We thank N. A. Cherepkov for stimulating discussion and collaboration. G.R. thanks H. C. Siegmann for continuous support.

- <sup>1</sup>L. Baumgarten, C.M. Schneider, H. Petersen, F. Schafers, and J. Kirschner, *Phys. Rev. Lett.* **65**, 492 (1990).
- <sup>2</sup>Ch. Roth, F.U. Hillebrecht, H. Rose, and E. Kisker, *Phys. Rev. Lett.* **70**, 3479 (1993); *Solid State Commun.* **86**, 647 (1993).
- <sup>3</sup>G. van der Laan, M.A. Hoyland, M. Surman, C.F. J. Flipse, and B.T. Thole, *Phys. Rev. Lett.* **69**, 3827 (1993).
- <sup>4</sup>F. Sirotti and G. Rossi, *Phys. Rev. B* **49**, 15 682 (1994).
- <sup>5</sup>G. Rossi, F. Sirotti, N. Cherepkov, F. Combet Farnoux, and G. Panaccione, *Solid State Commun.* **90**, 557 (1994).
- <sup>6</sup>G. Rossi, F. Sirotti, and G. Panaccione, in *Core Level Spectroscopies For Magnetic Phenomena: Theory and Experiment*, Vol. 345 of *NATO Advanced Study Institute, Series B: Physics*, edited by P.S. Bagus, G. Pacchioni, and F. Parmigiani (Plenum, New York, 1995).
- <sup>7</sup>H. Ebert, L. Baumgarten, C.M. Schneider, and J. Kirschner, *Phys. Rev. B* **44**, 4406 (1991).
- <sup>8</sup>D. Venus, *Phys. Rev. B* **49**, 8821 (1994).
- <sup>9</sup>G. van der Laan, *Phys. Rev. B* **51**, 240 (1995).
- <sup>10</sup>E. Tamura, G.D. Waddill, J.G. Tobin, and P.A. Sterne, *Phys. Rev. Lett.* **73**, 1533 (1994).
- <sup>11</sup>N.A. Cherepkov, *Phys. Rev. B* **50**, 13 813 (1994).
- <sup>12</sup>F. Sirotti, G. Panaccione, and G. Rossi, *Phys. Rev. B* **52**, R17 063 (1995).
- <sup>13</sup>N.A. Cherepkov, V.V. Kuznetsov, and V.A. Verbitskii, *J. Phys. B* **28**, 1221 (1995).
- <sup>14</sup>G. Rossi, G. Panaccione, F. Sirotti, and N. Cherepkov, *Phys. Rev. B* **55**, 11 483 (1997).
- <sup>15</sup>M. Getzlaff, Ch. Ostertag, G.H. Fecher, N. A. Cherepkov, and G. Schönhense, *Phys. Rev. Lett.* **73**, 3030 (1994).
- <sup>16</sup>G. Panaccione, F. Sirotti, E. Narducci, and G. Rossi, *Phys. Rev. B* **55**, 389 (1997).
- <sup>17</sup>G. Rossi, G. Panaccione, F. Sirotti, and N.A. Cherepkov, *Surf. Sci.* (to be published).
- <sup>18</sup>P. Bagus (unpublished).
- <sup>19</sup>B. T. Thole and G. van der Laan, *Phys. Rev. B* **44**, 12 424 (1991).
- <sup>20</sup>G. Rossi, F. Sirotti, and G. Panaccione, in *Magnetic Ultrathin Films, Multilayers and Surfaces*, edited by A. Fert *et al.*, MRS Symposia Proceedings No. 384 (Materials Research Society, Pittsburgh, 1995), p. 447.
- <sup>21</sup>F.U. Hillebrecht, Ch. Roth, H.B. Rose, W.G. Park, E. Kisker, and N.A. Cherepkov, *Phys. Rev. B* **53**, 12 182 (1996).
- <sup>22</sup>ELETTRA laboratory beamline handbook (1995).
- <sup>23</sup>S. Doniac and M. Sunjic, *J. Phys. C* **3**, 285 (1970).
- <sup>24</sup>J. C. Fuggle, F. U. Hillebrecht, R. Zeller, Z. Zolnierrek, P. A. Bennett, and Ch. Freiburg, *Phys. Rev. B* **27**, 2145 (1982); F. U. Hillebrecht, J. C. Fuggle, P.A. Bennett, Z. Zolnierrek, and Ch. Freiburg, *ibid.* **27**, 2179 (1982).
- <sup>25</sup>C.T. Chen, Y. U. Idzerda, H.-J. Lin, N.V. Smith, G. Meigs, E. Chaban, G.H. Ho, E. Pellegrin, and F. Sette, *Phys. Rev. Lett.* **75**, 152 (1995); B. T. Thole, P. Carra, F. Sette, and G. van der Laan, *ibid.* **68**, 1943 (1992); P. Carra, B. T. Thole, M. Altarelli, and X. Wang, *ibid.* **70**, 694 (1993).
- <sup>26</sup>F. Sirotti, M. De Santis, and G. Rossi, *Phys. Rev. B* **48**, 8299 (1993).